Journal of Mechanical Engineering Research and Developments
ISSN: 1024-1752
CODEN: JERDFO
Vol. 43, No. 5, pp. 318-331
Published Year 2020

Computational Investigation on Free and Forced Convection inside an Enclosure

Ali Abd Al-Nabi Abaas[†], Hasanen Mohammed Hussain[‡], Ali Najim Abdullah Saieed[‡†], Laith Jaafer Habeeb[‡‡], Humam Kareem Jalghaf[‡‡†]

[†]Mustansiriyah University / Government Contracts Division, Baghdad, Iraq
[‡]University of Technology, Mechanical Engineering Department.
[‡†]Al Rafidain University College, Department of Air-Conditioning and Refrigeration Eng. Tech., Baghdad, Iraq.
[‡‡]University of Technology / Training and Workshops Center
[‡‡†]Mechanical Eng. Dept. University of Technology, Baghdad, Iraq

*Corresponding Author Email: ali.alwalaa@gmail.com, hasanen.alsaady@yahoo.com, Ali.Najem@ruc.edu.iq, 20021@uotechnology.edu.iq, 20310@uotechnology.edu.iq

ABSTRACT: Enclosure with an inlet at the base and an opposite outlet at the top was investigated numerically using finite element method. The heat was applied to the sidewall of the enclosure away from the inlet opening. The Richardson number was changed a number by the values (0, 1, 2.5, 5, and 10). For each Richardson number, Reynold number was changed into (25, 50, 100, 200, 300, 400, and 500) respectively. Average and local Nusselt number was determined during the investigation as well as the streamlines and the isothermal patterns. The results revealed that as value increases of Reynolds number in the enclosure the Nusselt number was also increased, the same way as Richardson number increased the Nusselt number in the enclosure increased.

KEYWORDS: Enclosure, Numerical investigation, Nusselt number, Mixed convection.

INTRODUCTION

In the enclosures, the free convective heat transfer with heated isothermal walls has been a highly researched field because of its natural incidence in numerous real-world implementations, for example: solar energy flat-plate collectors, double-glazed windows, building enclosures, and nuclear reactors. Most of the research studied in this area is restricted to cases wherein the enclosure has vertical case (when the enclosure have gradient of a temperature is orthogonal to the gravity) or the enclosure have horizontal case (where the gradient of a temperature that aligns with gravity) to investigate of thermal instability or the traditional convection trouble respectively [1]. There were many studies like theoretical, numerical, and experimental researches aimed at getting a moderate or low Rayleigh number of the natural convection in inclined enclosures, numerous of these have predominating also suggested interconnection equations for Nusselt number in expressions of the studied variables. Motlagh et al. [2] studied the designing of the free convection of 2-phase Nano-fluid inside the tilted porous semi annulus enclosure. The water magnetic Nano-fluid cavity with (Fe_3O_4) is used to fill the enclosure. Darcy and Buongiorno samples were utilized for designing two-phase and then utilized for modeling porous media. In the case of low porous Rayleigh numbers, they found the Nusselt number (Nu) is not the job of the propensity angle and the porosity of the enclosure. In addition, when adding the nanoparticles volume fraction, the Nusselt number will increases. However, when pored Rayleigh numbers are high, the rate of heat transfer was decreasing via increasing the propensity angle of the enclosure. Moreover, the Nusselt number was increased when the value of the porosity increases. Pal et al. [3] investigated the Conjugate heat transfer caused by the combined conduction and convection of a (Cu-water) Nano-fluid in the case of a thick wall enclosure based on the non-homogeneous sample for the Nano-fluids. The results showed that the effect of the nanoparticles dispersion on the mixed convection was evident for a higher domain of the Richardson number (Ri) and the size fraction of nanoparticle. Both of the entropy generation and heat transfer improves at increasing the value of wave number and wave amplitude. Pandey et al. [4] extensively studied Natural convection because of its existence in numerous engineering applications. It is a very important method of heat transfer and which results because of the buoyancy induced flows caused by temperature variances. Their review displays of experimental and numerical studies attached to laminar natural convection in the enclosures for both states with and without interior objects. The influences on the thermal areas and flow system of different variables have been debated in detail, containing the number of internal bodies, aspect ratio, Rayleigh number, inclination angle, and position of internal bodies. Rehman et al. [5] studied the enclosure have trapezium shape where the fluid was driven via combine Buoyant convection influence. The left wall was assumed at an adiabatic stipulation and the upper wall with a cold state. He considered both of the bottom and right walls uniformly with non-uniformly heated case wise. The gotten results were displayed in the expression of streamlines and isotherms through a wide domain of Rayleigh number. The speed differences in expressions of (X) and (Y) components were specified for the walls with both states uniform and non-uniform heated. Yu-Shu Shi et al. [6] numerically investigated the forced flow body and mixed convection in the enclosure have a ventilated porous with a local tainted source on the floor at the position of floor center of the floor. Streamlines were created to show the forced flow body conversion from eddy free movement to the multi-eddy style. Akbar et al. [7] numerically studied the transport of particles in the laminar flow of free convection of air in the square shape of enclosures utilizing the Eulerian-Lagrangian method. The results showed that for the cases of low Rayleigh number the dispersion of the particles towards the walls, whereas the fraction of the particles were restricted in a near steady recirculation region. Furthermore, the results proved the important function of Brownian dispersion and thermo-apheresis, in particular for particles at the sub-micron size. Bastiaans et al. [8] investigate the flow of free convection created by a line heat exporter in restricted geometry. The purpose of the investigation is to scout the flow with the assist of numerical emulations. For the numerical emulation techniques, Large-Eddy Simulation (LES) and Direct Numerical Simulation (DNS) were employed. The three-dimensional simulation detected asymmetric time means recirculation that casings the range overhead the heat source. Cui et al. [9] studies the free convection in a section-triangular prismatic enclosure with different aspect ratios was conducted using three-dimensional numerical modeling approach. The flow structure of transverse rolls and longitudinal rolls was described. The critical Rayleigh numbers for the transition of the flow from driven by the baroclinic to Rayleigh-Bénard instability and from a steady to an unsteady state have been obtained for different aspect ratios. Garoosi et al. [10] conducted a parametric study to investigate the precipitation particle on surfaces of solid through the flow of free convection in an interior heated and cooling square cavity loaded with air. By utilizing the Eulerian-Lagrangian method, the trouble was numerically investigated. The 2D energy equations and Navier–Stokes were calculated utilizing the limit size discretization method. Furthermore, it was noted that by changing the HACs direction from vertical to horizontal and increasing the HACs number, increasing the precipitation average of the solid particles significantly. Asl et al. [11] performed a numerical analysis to investigate 2D natural convection into the heated tilted rectangular enclosure with many pored fins connected to the hot wall. The cavity was loaded with a Newtonian fluid incompressible, Fins are connected to the vertical wall with the hot state. Because of a small temperature variance between the cold and hot vertical walls, all of the thermo-physical features, which were shaped utilizing the Boussinesq approximation, are supposed constant. It was found that rising heat transfer utilizing very more fins that are porous relies upon the proportional thermal conductivity. The optimum length of the porous fin was found to be a reducing role of Rayleigh number. Luo et al. [12] numerically investigated the electro-thermal convection of a completely segregating liquid lie between a heated inner circular cylinder and a square enclosure utilizing a conjoined lattice Boltzmann method. Four equations of lattice Boltzmann were utilized to calculate all-controlling equations comprising a simplified group of Maxwell's equations, the power preservation equation, and the Navier-Stokes equations. It was found that the heat transfer increment caused by the influence of electrical becomes considerable when the electric leading parameter (T) above a critical sill. In this paper, the enclosure was studied by applying heat to one of its walls, the Nusselt number was investigated as well as the streamlines and the isothermal patterns, numerical finite element method was used for the investigation.

NUMERICAL METHOD

The schematic diagram of the problem shown in Figure 1 illustrate that the enclosure analyzed in this paper consist of a 2-D square cavity with an inlet opening and outlet, the wall on the far side of the opening is heated externally at constant temperature while the other walls are set as insulated walls. Galerkin finite element approach was used for numerical analysis, the non-dimensional governing equations solved by the model were as follows:

The continuity equation:

$$\frac{\partial u}{\partial x}+\frac{\partial \upsilon}{\partial y}=0 \tag{1}$$

X-Momentum equation:

$$u\frac{\partial u}{\partial x}+\upsilon\frac{\partial u}{\partial y}=-\frac{\partial p}{\partial x}+\frac{1}{\mathrm{Re}}\left(\frac{\partial^2 u}{\partial x^2}+\frac{\partial^2 u}{\partial y^2}\right) \tag{2}$$

Y-Momentum equation:

$$u\frac{\partial \upsilon}{\partial x}+\upsilon\frac{\partial \upsilon}{\partial y}=-\frac{\partial p}{\partial y}+\frac{1}{\mathrm{Re}}\left(\frac{\partial^2 \upsilon}{\partial x^2}+\frac{\partial^2 \upsilon}{\partial y^2}\right)+RiT \tag{3}$$

Energy equation:

$$u\frac{\partial T}{\partial x}+\upsilon\frac{\partial T}{\partial y}=\frac{1}{\mathrm{Re.Pr}}\left(\frac{\partial^2 T}{\partial x^2}+\frac{\partial^2 T}{\partial y^2}\right) \tag{4}$$

Where, (u), (υ) are the dimensionless horizontal and vertical velocity components along (X) and (Y) directions respectively, and (T), (p) are the dimensionless temperature and pressure.

The main governing parameters are:

Reynolds number (Re), Richardson number (Ri), and Prandtl number (Pr), they defined as:

$$\mathrm{Re}=\frac{\upsilon_{in}L}{v} \tag{5}$$

$$Ri=\frac{Gr}{\mathrm{Re}^2} \tag{6}$$

$$Gr=\frac{g.\beta.L^3(T_h-T_{in})}{v^2} \tag{7}$$

$$\mathrm{Pr}=\frac{v}{\alpha} \tag{8}$$

Where, (α), (ν), and (ρ) are the thermal diffusivity, kinematic viscosity and density of the fluid, and (g), (β) are the gravitational acceleration and the volumetric expansion coefficient. In this study the Prandtl number (Pr) for air set as 0.71, the ratio between the opening to the length of the enclosure S/L = 0.2. The computational domain in this method is normally subdivided roughly into a series of (448) separate macro-elements, as manifested in Figure (2). Then, the interior nodes to each macro-element can be generated within the run and spread according to the Gauss-Legendre-Lobatto quadrature. So, the simulation accuracy can be enhanced via increasing the polynomial order, (N×N), where (N) is the interior nodes number of the quadrature.

VALIDATION

The numerical model used to simulate the enclosure was validated using Angirasa [13]. Angirasa examined in detail the buoyancy interacted with the forced convection. Angirasa observed anomalous heat transfer behavior where the interaction becomes quite complex at higher absolute values of the Grashof number. Figure (3) shows a comparison between local Nusselt number along the hot wall for Angirasa results and the present results aimed at the case of Opposing flow. A good approximation was found between Angirasa results and the results of the current paper. The vortices transport equations and discretized power are together calculated utilizing the alternating direction implicit, and the stream assignment equation is calculated with the successive over-relaxation method. The validation took place at the following parameters, Grashof number = 10^6 , Prandtl number =0.7, Richardson number = 10. Which means Reynolds number = 316.22776

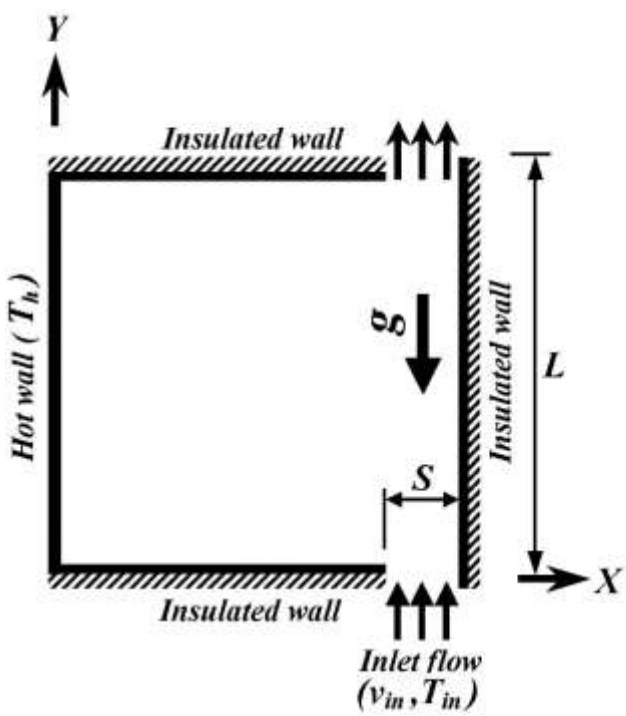

Figure 1: The physical domain of the current study.

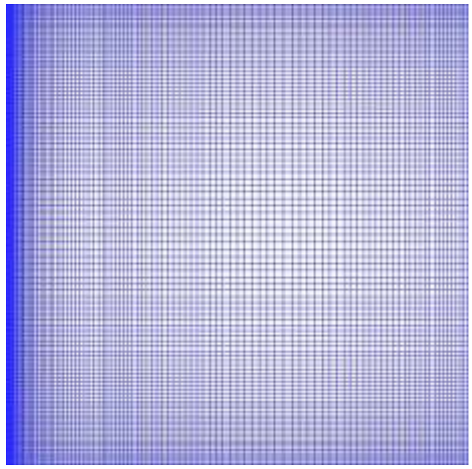

Figure 2: The meshing of the computational domain.

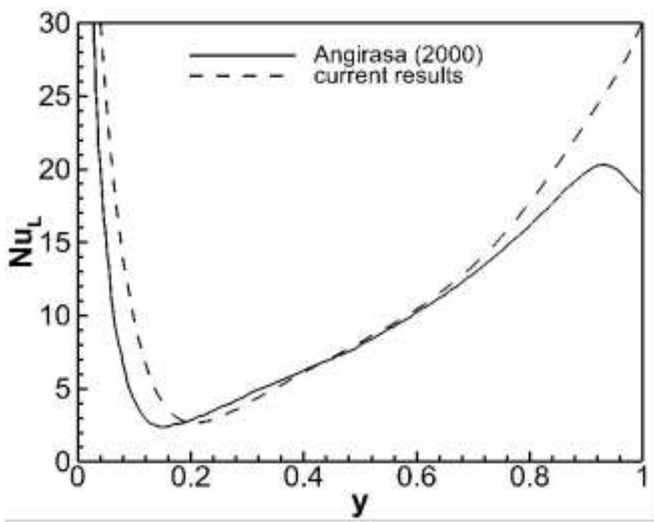

Figure 3: The validation of the current CFD results with the results of Angirasa [13].

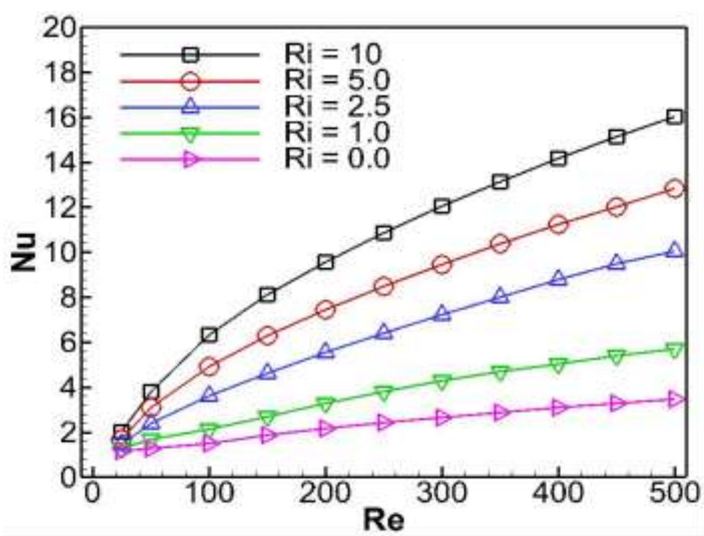

Figure 4: Variation of the average Nusselt number with the Reynolds number for different Richardson numbers.

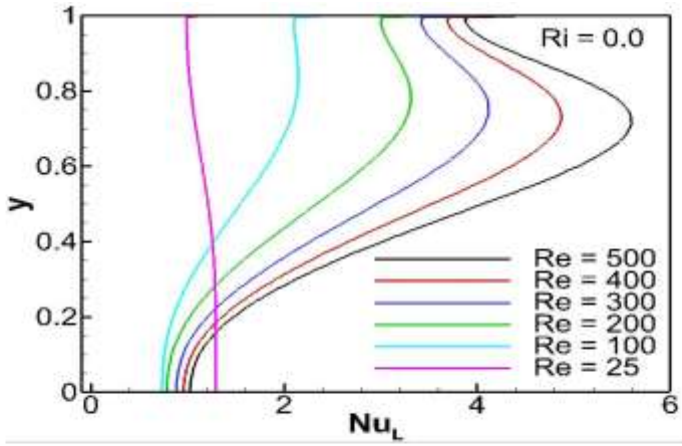

Figure 5: The local Nusselt number distributions along the heated wall at Ri = 0 and different Reynolds numbers.

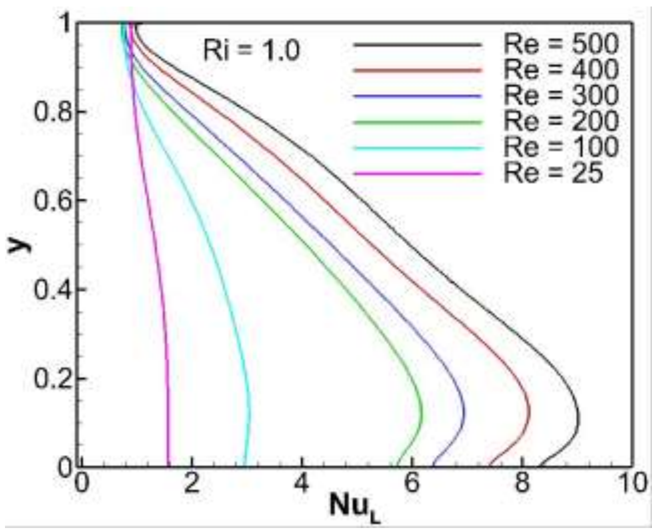

Figure 6: Local Nusselt number distributions along the heated wall at Ri = 1.0 and different Reynolds numbers.

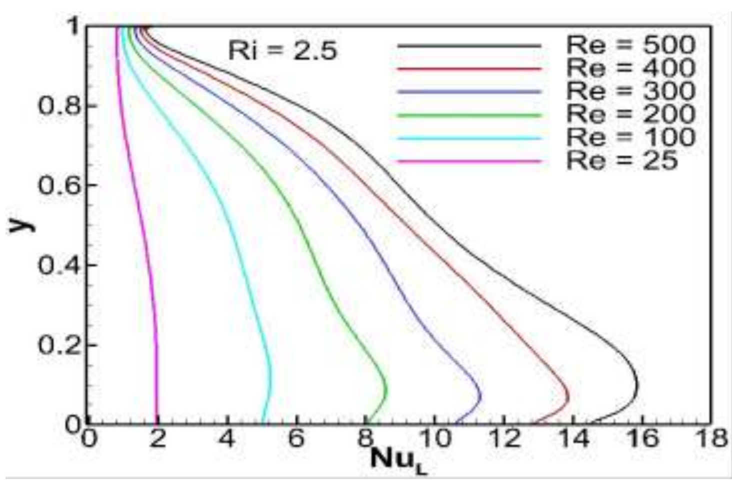

Figure 7: Local Nusselt number distributions along the heated wall at Ri = 2.5 and different Reynolds numbers.

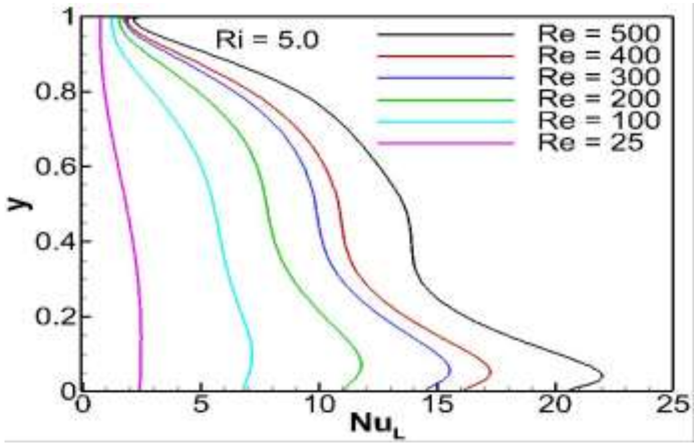

Figure 8: Local Nusselt number distributions along the heated wall at Ri = 5.0 and different Reynolds numbers.

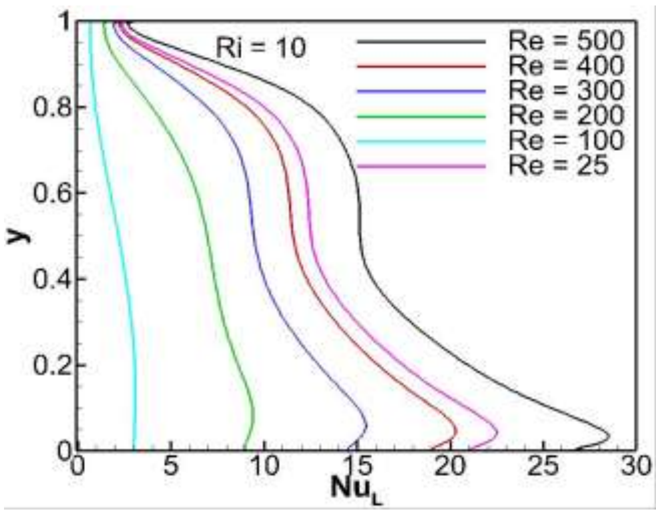

Figure 9: Local Nusselt number distributions along the heated wall at Ri = 10 and different Reynolds numbers.

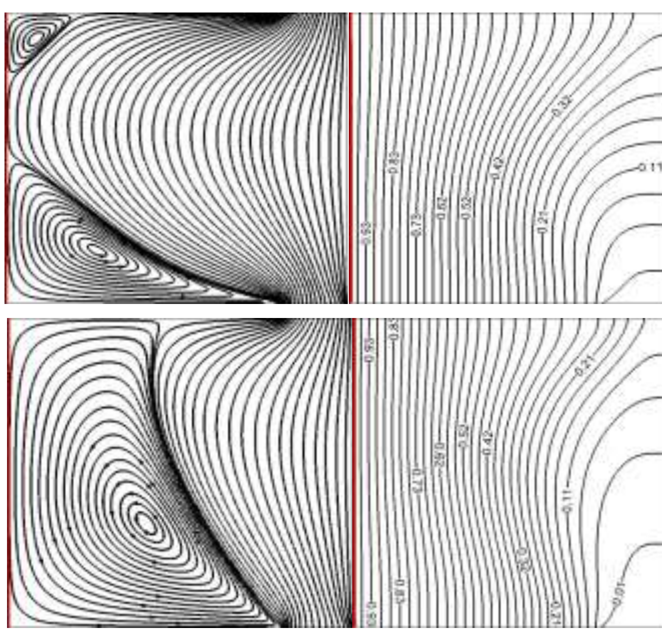

(a) Re = 25

(b) Re = 50

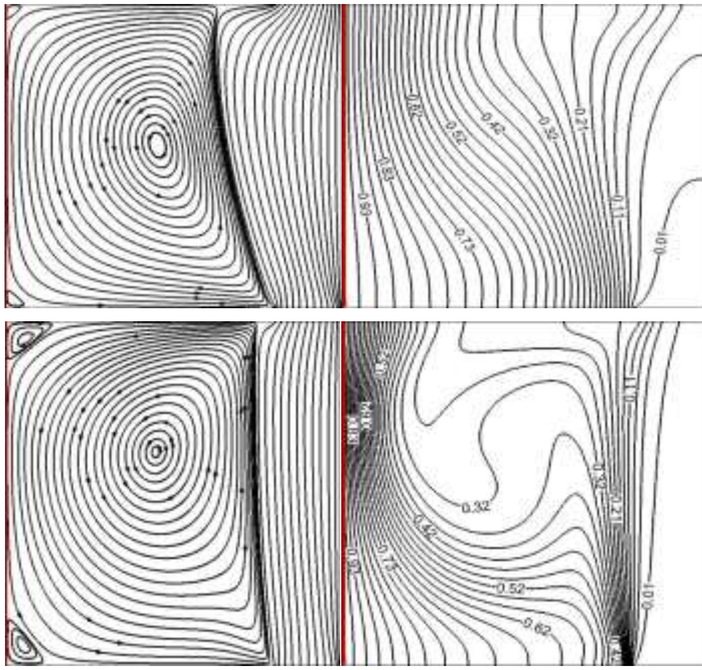

(c) Re = 100

(d) Re = 500

Figure 10: The streamline (left) and isotherm (right) patterns for mixed convective flow at different Reynolds numbers (a) Re=25, (b) Re=50, (c) Re=100, and (d) Re=500 and at Ri=0.0 (No Heating).

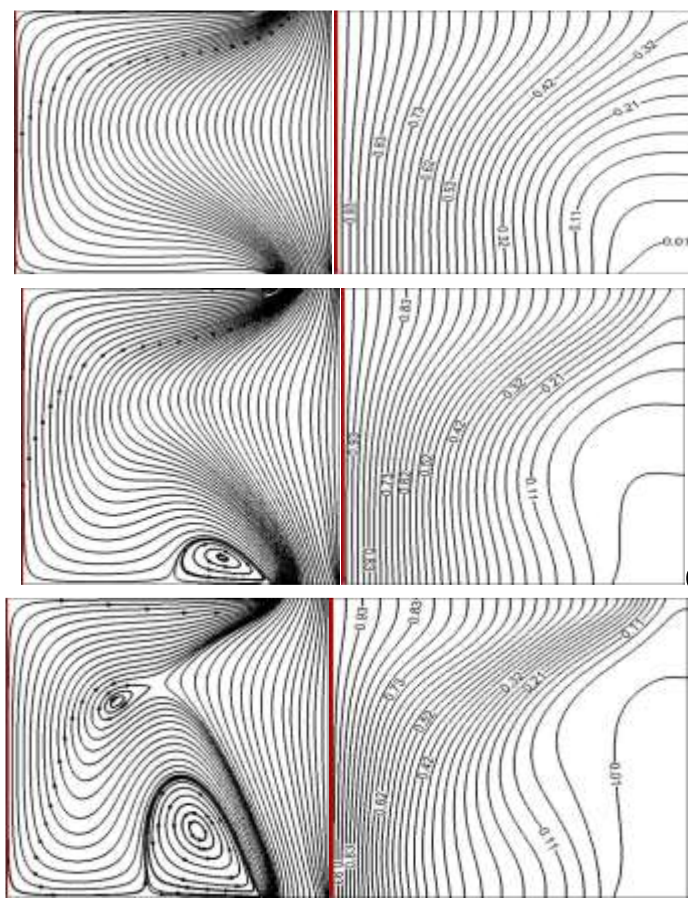

(a) Re=25

(b) Re=50

(c) Re=100

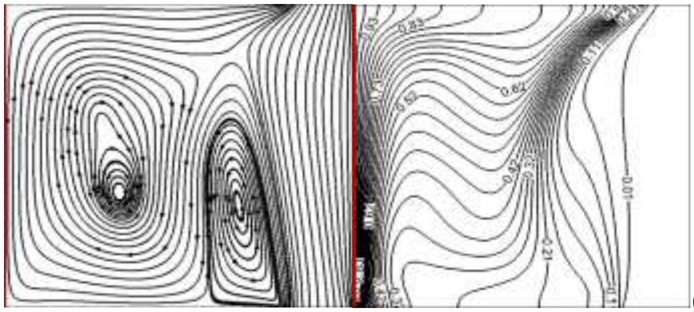
(d) Re=500

Figure 11: Streamline (left) and isotherm (right) patterns for mixed convective ow at different Reynolds number (a) Re=25, (b) Re=50, (c) Re=100, and (d) Re=500 and at Ri=1.0 (Mild Heating).

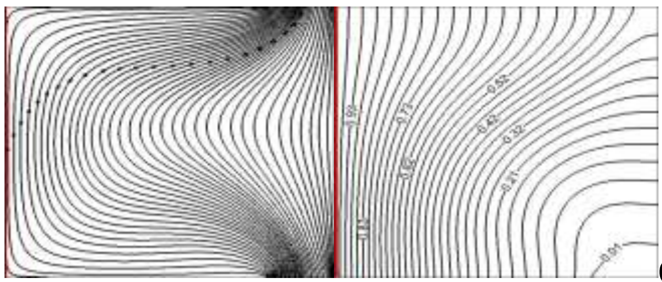
(a) Re=25

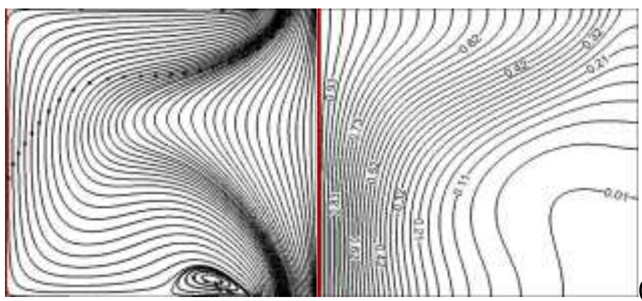
(b) Re=50

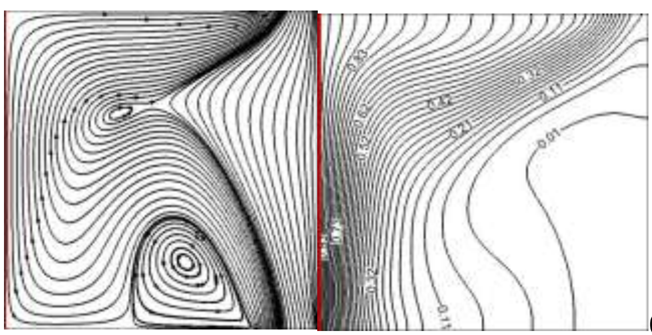
(c) Re=100

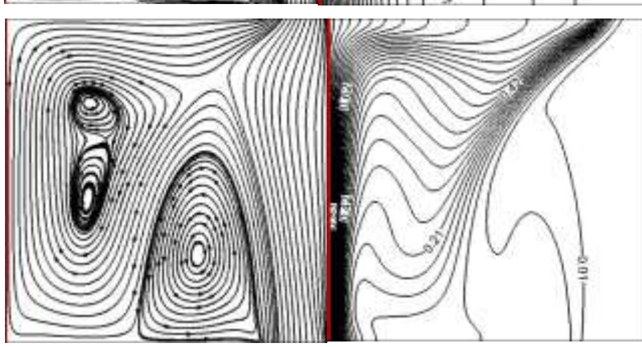
(d) Re=500

Figure 12: Streamline (left) and isotherm (right) patterns for mixed convective flow at different Reynolds number (a) Re=25, (b) Re=50, (c) Re=100, and (d) Re=500 and at Ri=2.5 (Moderate Heating).

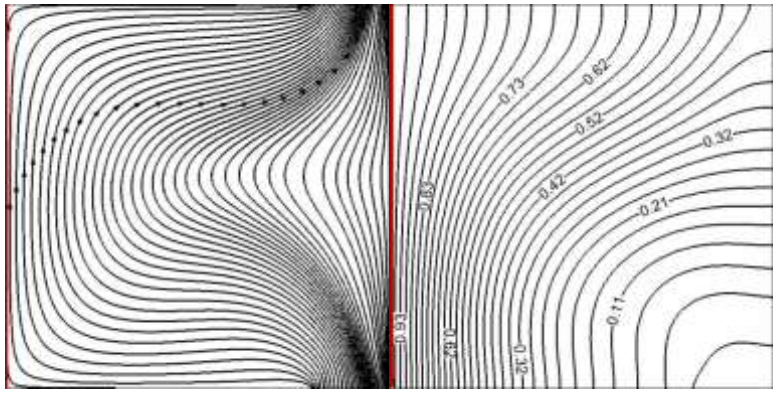

(a) Re=25

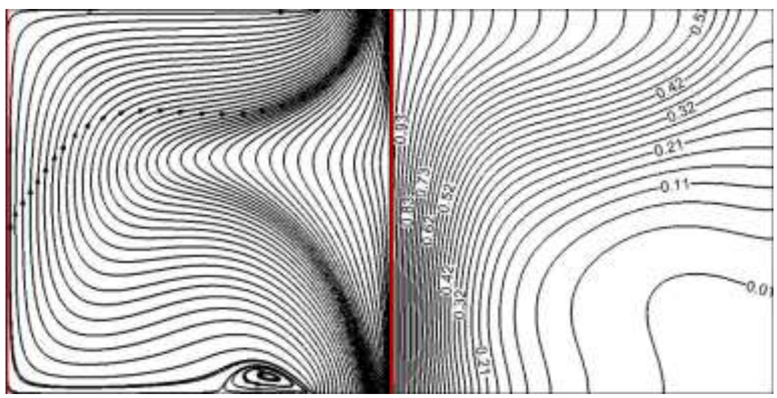

(b) Re=50

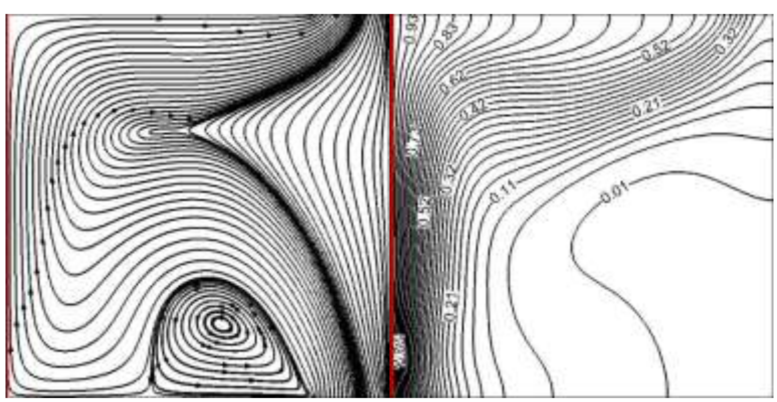

(c) Re=100

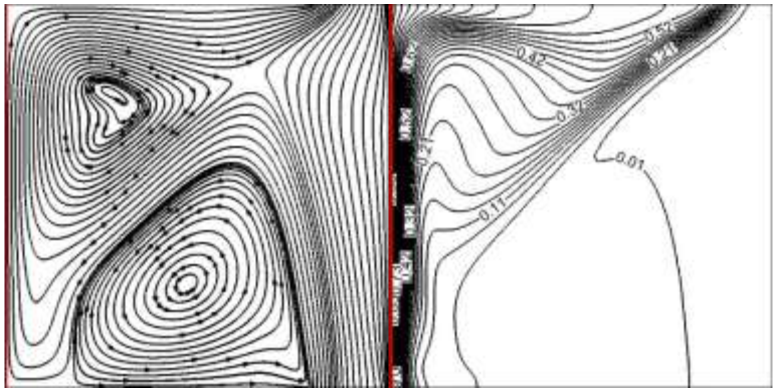

(d) Re=500

Figure 13: Streamline (left) and isotherm (right) patterns for mixed convective flow at different Reynolds number (a) Re=25, (b) Re=50, (c) Re=100, and (d) Re=500 and at Ri=5.0 (High Heating).

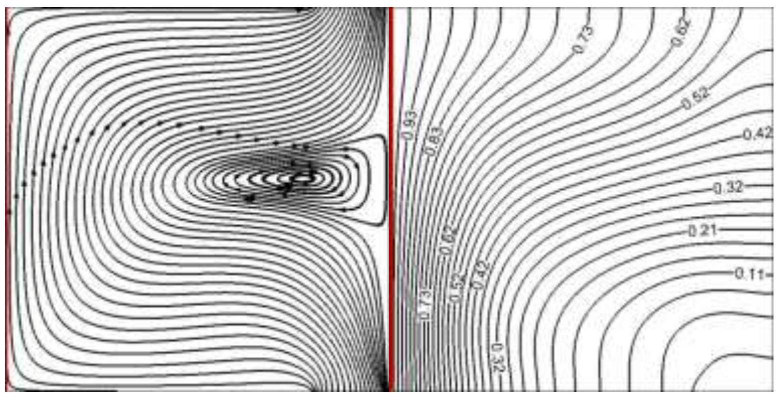

(a) Re=25

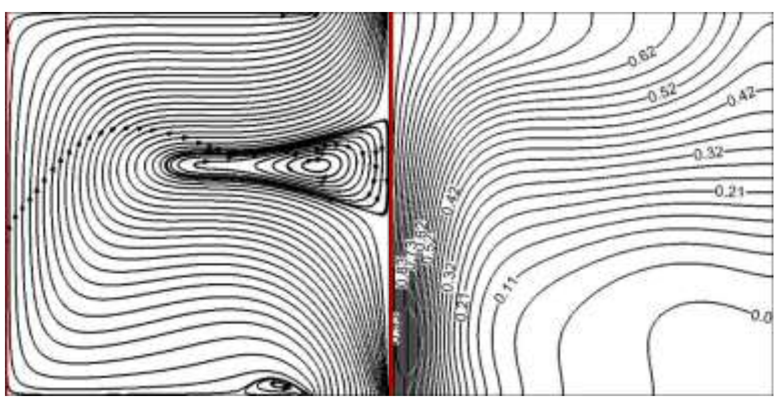

(b) Re=50

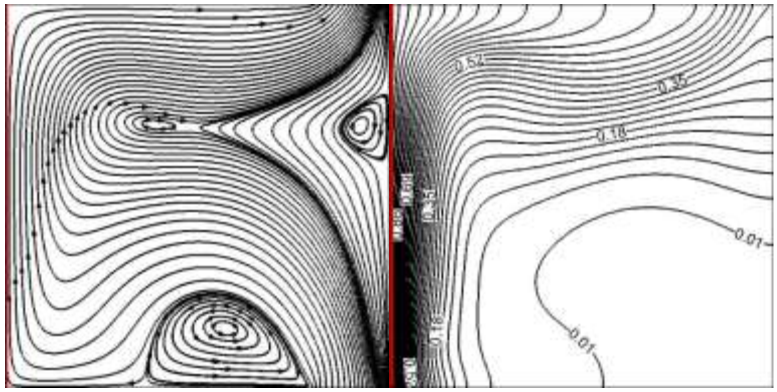

(c) Re=100

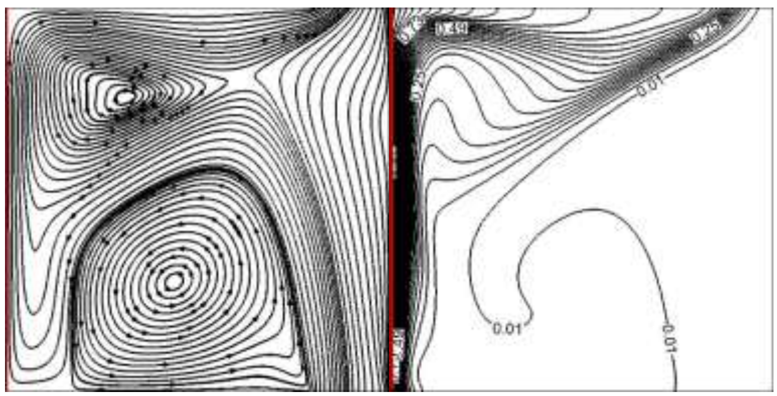

(d) Re=500

Figure 14: Streamline (left) and isotherm (right) patterns for mixed convective ow at different Reynolds number (a) Re=25, (b) Re=50, (c) Re=100, and (d) Re=500 and at Ri=10 (Huge Heating).

RESULTS AND DISCUSSION

Average Nusselt number variation with Reynolds number is shown in figure (4) through different values of the Richardson number. Figure (4) shows that Nusselt number increases as the value of Reynolds number increases, as Reynolds number was 33.3 Nusselt number was 0.8 for Richardson number of 0, as Reynolds number reaches 488.4 Nusselt number increases to 3.175 for Richardson number of 0. Figure (4) also shows the effect of Richardson number on the Nusselt number, when Richardson number increases the Nusselt number increases as well, for the same value of Reynolds number at Richardson number equal to 1.0 the Nusselt number was 3.6 then when Richardson number increased to 10 the Nusselt number increased as well to reach a value of 10.8. The heat transfer and thereby Nusselt number is highly influenced by the velocity and thereby Reynolds number, increasing the velocity in the enclosure increases the heat being transferred do to convection which explains the graph shown in figure (4).

Figures from (5) to (9) illustrate the local Nusselt number along the heated wall at various Reynolds number with values (25, 100, 200, 300, 400 and 500), and constant Richardson number. These figures illustrate the Nusselt number increasing throughout the wall and have a peak value and then start to decrease, for lower Reynolds number of 25, the Nusselt number was an almost a straight line from the start to the end of the wall. At a constant value of Richardson's number, the Reynolds number changed six times (25, 100, 200, 300, 400, and 500), for each figure from (5 to 9). These figures also illustrate that as Reynolds number increases the Nusselt number increases as well. As Richardson number changed with values of (0, 1, 2.5, 5 and 10), figure 4 to figure 8, the peak value starts to happened faster through the wall of the, cavity, then as Richardson number increase another peak value. From figure (9) at Richardson number equal to 10 and Reynolds number equal to 500 the first peak in Nusselt number was 28.58 at 0.03 on the wall, then the second one was 15 at 0.62 on the wall. The same effect was noticed for another Reynolds number, figure (5) shows at 25 Reynolds number the Nusselt number was an almost a straight line from the start of the heated wall to the end of it. At 500 Reynolds number, the Nusselt number start to increase from 1 at the beginning of the wall to a peak value of 5.6, then decreased to 3.9 at the end of the wall.

For mixed convection flow, the streamlines and isothermal patterns are shown in Figure (10) without heating, Richardson number 0, any wall of the enclosure. Richardson's number was 0 for all the tests with Reynolds number (25, 50, 100, and 500) respectively. At Reynolds number equal to 25 two small vortices were noted in the streamlined image from the Figure (10a). As Reynolds number increase to 50 the enclosure developed one large vortex, figure (10b) the streamline vortex starts to get bigger as the Reynolds number increases to 100, figure (10c). At Reynolds number 500, in addition to the big vortex developed throughout the enclosure two small vortices developed on the corners away from the inlet-outlet lines, see figure (10d). When a mild heat, Richardson number of value 1, goes through one of the cavity walls, the wall away from the inlet, streamline of the cavity changed. For Reynolds number of 25 there were no vortices in the enclosure, and then as Reynolds number increased, vortices start to develop near the inlet, see Figure (11). For moderate heat and high heat, Richardson number 2.5, and 5 respectively, as Reynolds number increases the vortices start to develop near the inlet of the enclosure, Figure (12, and 13). For huge heating, Richardson number 10, on the wall away from the cavity, Figure (14), as Reynolds number increases the vortices start to develop in the middle of the cavity away from the inlet-outlet line. The isothermal lines in Figure (14) show the heat starts to concentrate on the heated wall as the Reynolds number increases mean the convection in the flow starts to decrease as the velocity of the fluid increases.

CONCLUSION

Galerkin finite element method was used to study an enclosure. Varied values of Reynolds and Richardson's number were used to demonstrate their influence on the Nusselt number and the flow characteristic in the enclosure. The conclusions from this investigation are as follows:

1- The enclosure Nusselt number increase as the Reynolds number increase.

2- The enclosure Nusselt number increase as Richardson number increase, at the same value of Reynolds number.

3- The local Nusselt number along the heated wall increases with the increase in Reynolds and Richardson numbers

4- The streamlines of the enclosure changed with the amount of heat applied to the hot wall.

5- The isothermal lines show a concentration about the heated wall vicinity as Reynolds increases at constant Richardson number.

REFERENCES

[1] U. Madanan, and R.J. Goldstein, “Experimental investigation on very-high-Rayleigh-number thermal convection in tilted rectangular enclosures”, *International Journal of Heat and Mass Transfer*, Vol. 139, Pp. 121–129, 2019.

[2] S.Y. Motlagh, E. Golab, and A.N. Sadr, “Two-phase modeling of the free convection of Nano-fluid inside the inclined porous semi-annulus enclosure”, *International Journal of Mechanical Sciences*, Vol. 164, Pp. 105-183, 2019.

[3] S.K. Pal, S. Bhattacharyya, and I. Pop, "A numerical study on non-homogeneous model for the conjugate-mixed convection of a Cu-water Nano-fluid in an enclosure with thick wavy wall", *Applied Mathematics and Computation*, Vol. 356, Pp. 219–234, 2019.

[4] S. Pandey, Y.G. Park, and M.Y. Ha, "An exhaustive review of studies on natural convection in enclosures with and without internal bodies of various shapes", *International Journal of Heat and Mass Transfer*, Vol. 138, Pp. 762–795, 2019.

[5] K.U. Rehman, M.Y. Malik, M. Zahri, Q.M. Al-Mdallal, M. Jameel, and M.I. Khan, "Finite element technique for the analysis of buoyantly convective multiply connected domain as a trapezium enclosure with heated circular obstacle", *Journal of Molecular Liquids*, Vol. 286, Pp. 110-892, 2019.

[6] Y.S. Shi, D. Liu, Y. Wang, F.Y. Zhao, and Y.X. Li, "Forced flow structure and mixed convection in a ventilated porous enclosure with a local contaminant source", *International Journal of Heat and Mass Transfer*, Vol. 131, Pp. 973–983, 2019.

[7] M.K. Akbar, M. Rahman, and S.M. Ghiaasiaan, "Particle transport in a small square enclosure in laminar natural convection", *Aerosol Science*, Vol. 40, Pp. 747 – 761, 2009.

[8] Rob J.M. Bastiaans, C.C.M. Rindt, F.T.M. Nieuwstadt, A.A. van Steenhoven, "Direct and large-eddy simulation of the transition of two- and three-dimensional plane plumes in a confined enclosure", *International Journal of Heat and Mass Transfer*, Vol. 43, Pp. 2375-2393, 2000.

[9] H. Cui, F. Xu, S.C. Saha, and Q. Liu, "Transient free convection heat transfer in a section-triangular prismatic enclosure with different aspect ratios", *International Journal of Thermal Sciences*, Vol. 139, Pp. 282–291, 2019.

[10] F. Garoosi, M.R. Safaei, M. Dahari, K. Hooman, "Eulerian–Lagrangian analysis of solid particle distribution in an internally heated and cooled air-filled cavity", *Applied Mathematics and Computation*, Vol. 250, Pp. 28–46, 2015.

[11] A.K. Asl, S. Hossainpour, M.M. Rashidi, M.A. Sheremet, Z. Yang, "Comprehensive investigation of solid and porous fins influence on natural convection in an inclined rectangular enclosure", *International Journal of Heat and Mass Transfer*, Vol. 133, Pp. 729–744, 2019.

[12] K. Luo, J. Wu, H.L. Yi, and H.P. Tan, "Numerical investigation of heat transfer enhancement in electro-thermo-convection in a square enclosure with an inner circular cylinder", *International Journal of Heat and Mass Transfer*, Vol. 113, Pp. 1070–1085, 2017.

[13] D. Angirasa, "Mixed convection in a vented enclosure with an isothermal vertical surface", *Fluid Dynamics Research*, Vol. 26, Pp. 219-233, 2000.